Localization transitions in an open quasiperiodic ladder

Suparna Sarkar,^{1,*} Soumya Satpathi,^{1,†} and Swapan K. Pati^{1,‡}

¹Theoretical Sciences Unit, School of Advanced Materials (SAMat),

Jawaharlal Nehru Centre for Advanced Scientific Research, Bangalore 560064, India

(Dated: November 12, 2025)

We investigate localization transition in an open quasiperiodic ladder where the quasiperiodicity is described by the Aubry-André-Harper model. While previous studies have shown that higher-order hopping or constrained quasiperiodic potentials can induce a mixed-phase zone in one dimension, we demonstrate that the dissipation can induce mixed phase zone in a one dimensional nearest-neighbor system without imposing any explicit constraints on the quasiperiodic potential or hopping parameter. Our approach exploits an exact correspondence between the eigenspectrum of the Liouvillian superoperator and that of the non-Hermitian Hamiltonian, valid for quadratic fermionic systems under linear dissipation. Using third quantization approach within Majorana fermionic representation, we analyze two dissipation configurations: alternating gain and loss at every site, and at alternate sites under balanced and imbalanced conditions. By computing the inverse and normalized participation ratios, we show that dissipation can drive the system into three distinct phases: delocalizd, mixed, and localized. Notably, the mixed-phase zone is absent for balanced dissipation at every site but emerges upon introducing imbalance, while for alternate site dissipation it appears in both balanced and imbalanced cases. Furthermore, the critical points and the width of the mixed-phase window can be selectively tuned by varying the dissipation strength. These findings reveal that the dissipation plays a decisive role in reshaping localization transitions in quasiperiodic systems, offering new insight into the interplay between non-Hermitian effects and quasiperiodic order.

I. INTRODUCTION

The phenomenon of localization in quantum systems has long been a subject of fundamental and practical interest since its prediction by P. W. Anderson in 1958¹. The pioneering work of Anderson demonstrates that in low-dimensional systems with uncorrelated site potentials, all energy eigenstates exhibit exponential localization, regardless of the disorder strength. It makes the system quite trivial one as no mobility edge (ME) exist to separate a conducting region from an insulating one, which is essential for a disorder-induced metal-toinsulator transition^{2,3}. However, In three-dimensional systems, disorder enables the coexistence of extended and localized states, separated by a ME at a critical energy⁴. In contrast to randomly disordered systems, a quasiperiodic system can exhibit a ME through a controllable metal-insulator phase transition even in low dimensions^{5,6}. A famous example is the Aubry-André-Harper (AAH)^{7,8} model, in which the on-site potentials follow a cosine modulation pattern. It exhibits a sharp transition where all eigenstates are delocalized below a critical point but become fully localized beyond it. Since the critical disorder strength does not depend on eigenenergy, there is no ME in such systems⁸. The emergence of mobility edge requires coupling of two one-dimensional AAH chains to construct a ladder, along with the presence of diagonal inter-chain couplings. The introduction of the diagonal hopping leads to the appearance of two separate transition points, giving rise to a mixed-phase zone, which is essential for the appearance of ME in the energy spectrum^{9,10}. In addition, energy-dependent MEs can be generated in 1D AAH models by incorporating long-range hopping 11,12, short-range dimerized hopping^{13,14}, or by engineering the structure of the quasiperiodic potentials $^{15-17}$.

Recently, the study of open quantum systems have

gained significant attention, since realistic quantum systems are inherently coupled to their surrounding environments. Such systems play a pivotal role across diverse fields, including chemistry, atomic and molecular physics, quantum optics, condensed matter physics, quantum information, and quantum computation ^{18–22}. Open quantum systems can be described using a non-Hermitian Hamiltonian, where physical gain and loss are captured by introducing imaginary terms into the Hamiltonian, and their properties are analyzed through the resulting complex eigenvalue spectrum^{23–26}. The non-Hermitian systems can show exotic phenomena such as non-Hermitian skin effect^{27–30}, parity-time (\mathcal{PT}) phase transition^{31–33}, and exceptional points^{34–36}. Moreover, open systems have been realized experimentally in various systems, including optical, mechanical, and electrical setups, which highlight the practical significance of non-Hermitian systems^{37–41}. Anderson localization has been explored in disordered optical lattice systems, revealing that the presence of physical gain and loss can enhance the localization of $light^{42,43}$. In addition, the role of \mathcal{PT} -symmetry in the non-Hermitian Aubry-André model has also received considerable attention^{44,45}. Despite significant progress, non-Hermitian Hamiltonians only describe the dynamics at short times, whereas the long-time, unconditional evolution is governed by the Liouvillian of the master equation 46-48. Although localization has been extensively studied in closed systems, and recent works have been addressed environmental effects through non-Hermitian Hamiltonians by introducing imaginary terms, a comprehensive understanding of localization in open quasiperiodic systems is still lacking. Exploring a Liouvillian-based framework is essential to reveal how both coherent dynamics and dissipation reshape localization transitions in realistic scenario.

To address this issue, we investigate the effect of environmental dissipation on localization properties of a

quasiperiodic two stranded ladder. In our approach, the essential features of non-Hermitian quasicrystals are incorporated into the dissipative quantum jump processes described by a Lindblad master equation. Within this framework, the long-time dynamical transitions are directly linked to the phase transitions of the corresponding non-Hermitian effective Hamiltonian. We introduce single-site Lindblad operators in two different configurations, applied to every site in one case and to alternating sites in the other, in order to examine the impact of distinct dissipation patterns. Using third quantization and calculating the bath matrices corresponding to dissipation in the Majorana fermionic representation, we obtain the system's damping matrix. From its eigenfunctions, we compute the inverse and normalized participation ratios to analyze the localization properties. Our results indicate that dissipation gives rise to a rich phase diagram with extended, mixed, and localized phases, where the mixed-phase window and critical point are tunable through the dissipation strength. Specifically, when dissipation acts on every sites under balanced gain-loss conditions, the localization transition occurs at a critical point same as closed AAH ladder and there is no mixed-phase zone. Introducing imbalance leads to the emergence of a mixed-phase zone, which broaden as imbalance increases. In contrast, when dissipation is applied to alternating sites, a mixed-phase zone arises even under balanced condition. In both the scenarios, the critical values of localization transition decreases with increasing imbalance between gain and loss. Interestingly, our results indicate that in presence of dissipation, a mixed-phase zone can emerge in a one-dimensional AAH ladder even in absence of diagonal hopping or without imposing any constraints on the quasiperiodic potential.

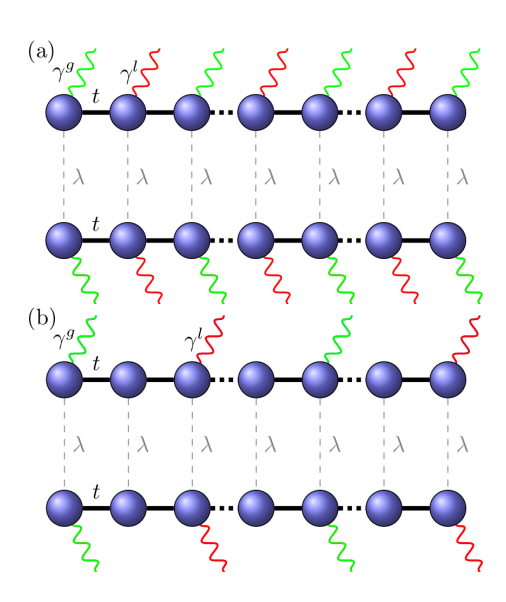


FIG. 1: (Color online). Schematic representation of two-stranded Aubry-André-Harper ladders illustrating two dissipation configurations: (a) alternating gain and loss at every site, and (b) alternating gain and loss applied at every other site. γ^g and γ^l denote the strengths of gain and loss dissipation, respectively, while t and λ represent the intra-chain and inter-chain hopping amplitudes, respectively.

The rest of the paper is structured as follows: Sec. II introduces the model, Hamiltonian, and the theoretical framework based on third quatization formalism within Majorana fermionic representation. In Sec. III, we present and analyze the results in detail. Finally, Sec. IV provides the conclusions.

II. MODEL AND METHODS

We consider a open quantum system of fermions in dissipative environment described by the Lindblad master equation 49,50

$$\frac{d\rho}{dt} = \hat{\mathcal{L}}\rho = -i[H, \rho] + \sum_{m} \left(L_{m}\rho L_{m}^{\dagger} - \frac{1}{2} \{ L_{m}^{\dagger} L_{m}, \rho \} \right),$$
(1)

where ρ is the density matrix, H is the system's Hamiltonian. $\hat{\mathcal{L}}$ denotes the Liouvillian superoperator and L_m are Lindblad operators represent the effect of different baths. From a quantum-trajectory viewpoint, in the absence of the quantum-jump contributions $L_m \rho L_m^{\dagger}$, the short-time evolution is governed by the effective non-Hermitian Hamiltonian $H_{\rm eff} = H_0 - i \sum_m L_m^{\dagger} L_m^{51,52}$. Conversely, the long-time evolution is determined by the Liouvillian superoperator \mathcal{L} , with the steady-state density matrix ρ_s satisfying $\mathcal{L}\rho_s = 0$.

If all L_m are linear in fermionic operator, the master equation generates quadratic Lindbladians. By applying third quantization approach^{53,54}, these quadratic Lindb-bladians can be diagonalized in the canonical basis of Majorana fermions. A single complex fermion can always be represented in terms of a pair of Majorana fermions, for instance

$$w_{2j-1} = (c_j + c_j^{\dagger}), \quad w_{2j} = i(c_j - c_j^{\dagger}),$$

satisfying the anti-commutation relation

$$\{w_i, w_k\} = 2\delta_{i,k}, \quad j, k = 1, 2, \dots, 2n.$$

Now the system's Hamiltonian and the bath operators can be written in the Majorana fermion basis as

$$H = \sum_{i,j} H_{ij} w_i w_j, \tag{2}$$

$$L_m = \sum_{j} l_{m,j} w_j. (3)$$

The Hilbert space is now mapped onto the 2^{2n} -dimensional Liouville space \mathcal{K} , which is spanned by the new set of Majorana operators $P_{\alpha} = w_1^{\alpha_1} w_2^{\alpha_2} \cdots w_{2n}^{\alpha_{2n}}$, where $\alpha_j \in \{0, 1\}$. In this canonical basis the Liouvillian of Eq. (1) contain both the even and odd parity subspaces and it can be written in the following bilinear form

$$\hat{\mathcal{L}} = \frac{1}{2} \sum_{i,j} \left(\hat{c}_i^{\dagger} \ \hat{c}_i \right) A_{ij} \begin{pmatrix} \hat{c}_j \\ \hat{c}_j^{\dagger} \end{pmatrix} - A_0 \hat{\mathbf{I}}, \tag{4}$$

This equation needs to define in two parity subspaces. Since, a physical observable contain even number of Majorana fermions operator, we can consider this equation in even subspaces only, in which the structure matrix $\bf A$ of dimension $4N \times 4N$ takes the form⁵⁵

$$\mathbf{A} = \begin{pmatrix} -\mathbf{X}^{\dagger} & -i\mathbf{Y} \\ 0 & \mathbf{X} \end{pmatrix}. \tag{5}$$

with

$$\mathbf{X} = -4i\mathbf{H} + 2\left(\mathbf{M} + \mathbf{M}^{T}\right),$$

$$\mathbf{Y} = -4i\left(\mathbf{M} - \mathbf{M}^{T}\right),$$

$$\mathbf{A_{0}} = \frac{1}{2}\text{Tr}\,\mathbf{X}.$$
(6)

M is a complex Hermitian matrix which provides the parametrization for the Lindblad operators

$$M_{ij} = \sum_{m} l_{m,i} l_{m,j}^*. (7)$$

The Hamiltonian matrix \mathbf{H} and the bath matrix \mathbf{M} , both have the dimensions $4N \times 4N$. Since, \mathbf{A} has a blocktriangular form, the spectrum of $\hat{\mathcal{L}}$ is fully determined by the eigenvalues β_i of matrix \mathbf{X} , called the rapidities. By calculating eigenvectors of \mathbf{A} , we can construct the normal master modes b_j , b'_j and the Liouvillian takes the diagonal form $\hat{\mathcal{L}} = \sum_j \beta_j b'_j b_j$. The eigenspectrum of X, contain all the information about liouvillian spectrum. It can be shown that, the eigenspectrum of the damping matrix and that of the non-Hermitian effective Hamiltonian contains the same information 56 .

As shown in Fig. 1, our system consist of a quasiperiodic two-stranded ladder with local baths having N lattice sites in each strand. We consider two different dissipation configurations: in the first, local gain and loss are applied alternately on every site, while in the second, they are applied alternatively on every other site. The tight-binding Hamiltonian of the ladder is given by

$$H = \sum_{p=I,II} \left[\sum_{j=1}^{N} \epsilon_{p,j} c_{p,j}^{\dagger} c_{p,j} + \sum_{j=1}^{N-1} t_{p} \left(c_{p,j}^{\dagger} c_{p,j+1} + c_{p,j+1}^{\dagger} c_{p,j} \right) \right] + \sum_{j=1}^{N} \lambda \left(c_{I,j}^{\dagger} c_{II,j} + c_{II,j}^{\dagger} c_{I,j} \right).$$
(8)

Here, p (= I, II) labels the strand index, while j denotes the lattice sites along each strand. The operators $c_{p,j}^{\dagger}$ and $c_{p,j}$ are the standard fermionic creation and annihilation operators, respectively. The parameter t_p represents the intra-strand hopping amplitude for strand p, and λ denotes the inter-strand coupling strength.

The parameter $\epsilon_{p,j}$ represents the on-site energy of an electron at site j of the strand p. Under the influence of AAH modulation, the on-site energies along both strands can be written as

$$\epsilon_{\text{I},j} = \epsilon_{\text{II},j} = V \cos(2\pi bj)$$
 (9)

where $b = (\sqrt{5} - 1)/2$.

For the bath, we choose single-site lindblad operators for gain and loss as:

$$L_{p,j}^{g} = \sqrt{\gamma^{g}} c_{p,j}^{\dagger};$$

$$L_{p,j}^{l} = \sqrt{\gamma^{l}} c_{p,j};$$
(10)

where γ^g and γ^l are the gain and loss strength respectively.

Now in Majorana fermion basis $w_{p,2j-1}=(c_{p,j}+c_{p,j}^{\dagger}); \quad w_{p,2j}=i(c_{p,j}-c_{p,j}^{\dagger})$ the Hamiltonian of Eq. (8) and the Lindblad operators of Eq. (10), can be written as

$$H = \sum_{p=1,\text{II}} \left[\frac{1}{2} \sum_{j=1}^{N} \epsilon_{p,j} (1 + i w_{p,2j} w_{p,2j-1}) + \frac{i t_p}{2} \sum_{j=1}^{N-1} \left(w_{p,2j} w_{p,2j+1} - w_{p,2j-1} w_{p,2j+2} \right) \right] + \frac{i \lambda}{2} \sum_{j=1}^{N} \left(w_{\text{I},2j} w_{\text{II},2j-1} - w_{\text{I},2j-1} w_{\text{II},2j} \right)$$
(11)

$$L_{p,j}^{g} = \frac{\sqrt{\gamma^{g}}}{2} (w_{p,2j-1} + iw_{p,2j})$$

$$L_{p,j}^{l} = \frac{\sqrt{\gamma^{l}}}{2} (w_{p,2j-1} - iw_{p,2j}). \tag{12}$$

We construct the bath matrix M using Eq. (7) and Eq. (12) in Majorana fermion basis. For dissipation at every site, the bath matrix takes the form

$$M = \frac{1}{4} \begin{pmatrix} \gamma^g & -i\gamma^g & 0 & 0 & 0 & 0 & 0 & 0 \\ i\gamma^g & \gamma^g & 0 & 0 & 0 & 0 & 0 & 0 & 0 \\ 0 & 0 & \gamma^l & i\gamma^l & 0 & 0 & 0 & 0 & 0 \\ 0 & 0 & -i\gamma^l & \gamma^l & 0 & 0 & 0 & 0 & 0 \\ & & & \ddots & & & & \\ 0 & 0 & 0 & 0 & \gamma^g & -i\gamma^g & 0 & 0 \\ 0 & 0 & 0 & 0 & i\gamma_g & \gamma_g & 0 & 0 \\ 0 & 0 & 0 & 0 & 0 & 0 & \gamma^l & \gamma^l \\ 0 & 0 & 0 & 0 & 0 & 0 & -i\gamma^l & \gamma^l \end{pmatrix}.$$

For dissipation applied at every other site, the bath matrix is given by

From Eq. (6), the corresponding damping matrix X can then be obtained by using the above bath matrices. To

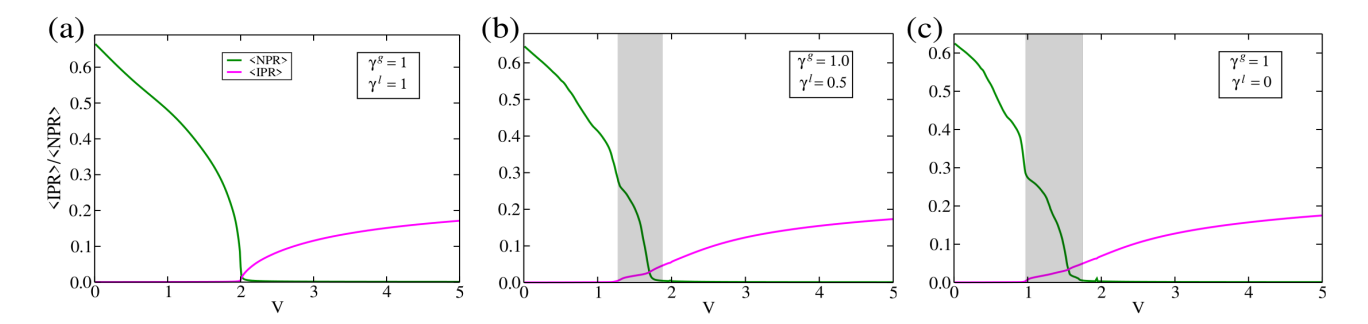


FIG. 2: (Color online). $\langle \text{IPR} \rangle$ and $\langle \text{NPR} \rangle$ as functions of the Aubry-André-Harper disorder strength, with dissipation applied at every site. Panels (a)–(c) correspond to: (a) $\gamma^g=1$, $\gamma^l=1$; (b) $\gamma^g=1$, $\gamma^l=0.5$; and (c) $\gamma^g=1$, $\gamma^l=0$. Here the system size is 2N=3000.

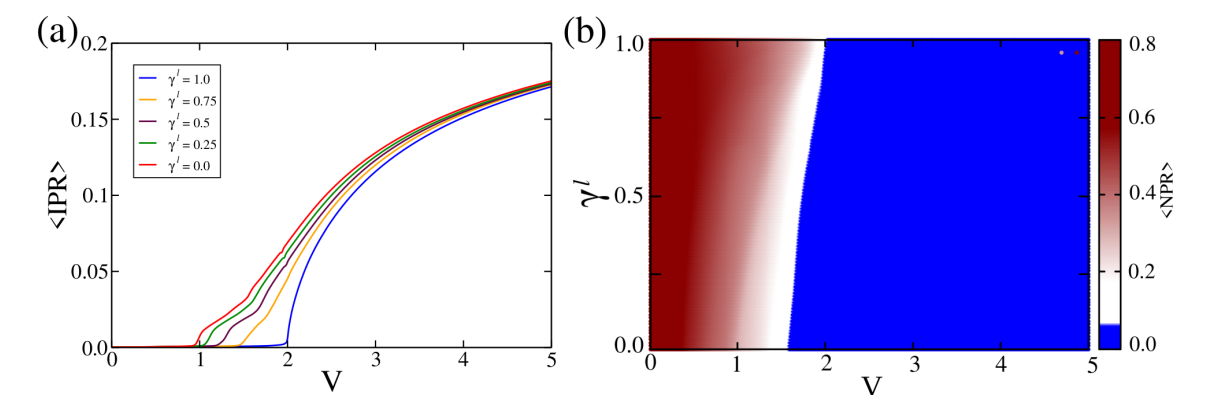


FIG. 3: (Color online). With dissipation applied at every site: (a) $\langle IPR \rangle$ as a function of the Aubry-André-Harper disorder strength V for $\gamma^l = 1, 0.75, 0.5, 0.25$, and 0, with fixed $\gamma^g = 1$ and system size 2N = 3000. (b) Phase diagram in the parameter space spanned by V and γ^l , where the color bar represents the $\langle NPR \rangle$. Here $\gamma^g = 1$ and the system size is 2N = 500.

see the impact of dissipation on localization transitions, we analyze the properties of the eigenstates of the damping matrix. If $|\psi_n\rangle$ is the normalized eigenstate of nth state and 4N is the dimension of the damping matrix X, then the degree of localization can be quantified using inverse participation ratio (IPR) and normalized participation ratio (NPR) defined as

$$IPR_n = \frac{\sum_{j=1}^{4N} |\psi_{n,j}|^4}{\left(\langle \psi_n | \psi_n \rangle\right)^2}$$
(13)

and

$$NPR_n = (4N \times IPR_n)^{-1} \tag{14}$$

In thermodynamic limit, for a delocalized eigenstate IPR= 0 and NPR \neq 0, whereas for a localized eigenstate, IPR \neq 0 and NPR= 0. To gain a comprehensive understanding of the spectrum, we evaluate the average IPR and NPR by summing over all eigenstates, defined as follows.

$$\langle IPR \rangle = \frac{1}{4N} \sum_{n=1}^{4N} IPR_n$$
 (15)

and

$$\langle \text{NPR} \rangle = \frac{1}{4N} \sum_{n=1}^{4N} \text{NPR}_n$$
 (16)

III. NUMERICAL RESULTS AND DISCUSSION

Based on the above theoretical prescription now we present our essential results. The main focus is to discuss the intricate interplay between dissipation and quasiperiodicity on localization transition of AAH ladder. We will consider two configurations: (i) dissipation at every site, and (ii) dissipation at alternate sites. The balanced and imbalanced condition can be tuned by varying the relative strengths of loss and gain. For both these cases we critically analyze the effect of dissipation strength on critical point and mixed-phase zone. The values of parameters which are kept constant throughout the calculations are: intra-chain hopping $t_{\rm I} = t_{\rm II} = 1$, inter-strand hopping $\lambda = 1$, and unless stated otherwise each strand consists of a total of N = 1500 lattice sites.

A. Dissipation at every site

In this case, each site is subject to dissipation, with the Lindblad operators acting alternately as gain and loss. Specifically, the gain and loss operators are acting as:

$$\begin{split} L_{p,j}^g &= \sqrt{\gamma^g} c_{p,j}^\dagger; & \quad \text{for odd j} \\ L_{p,j}^l &= \sqrt{\gamma^l} c_{p,j}; & \quad \text{for even j} \end{split}$$

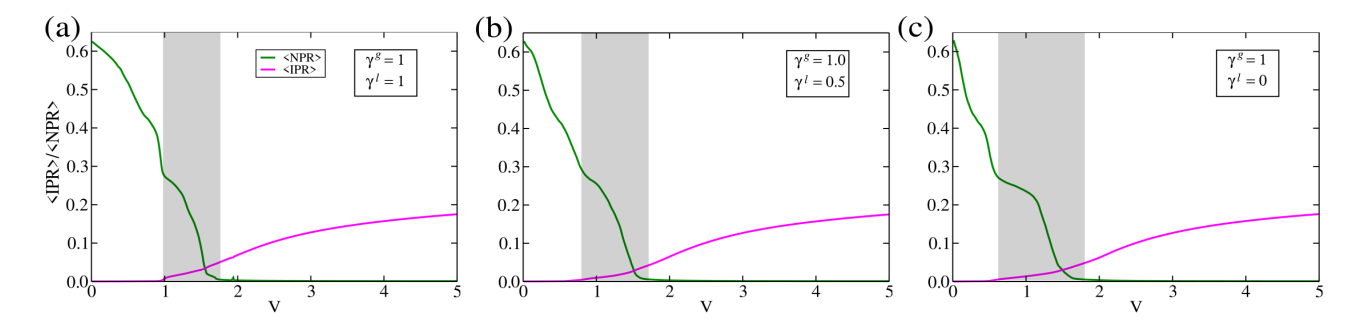


FIG. 4: (Color online). $\langle \text{IPR} \rangle$ and $\langle \text{NPR} \rangle$ as functions of the Aubry-André-Harper disorder strength, with dissipation applied at alternate site. Panels (a)–(c) correspond to: (a) $\gamma^g=1$, $\gamma^l=1$; (b) $\gamma^g=1$, $\gamma^l=0.5$; and (c) $\gamma^g=1$, $\gamma^l=0$. Here the system size is 2N=3000.

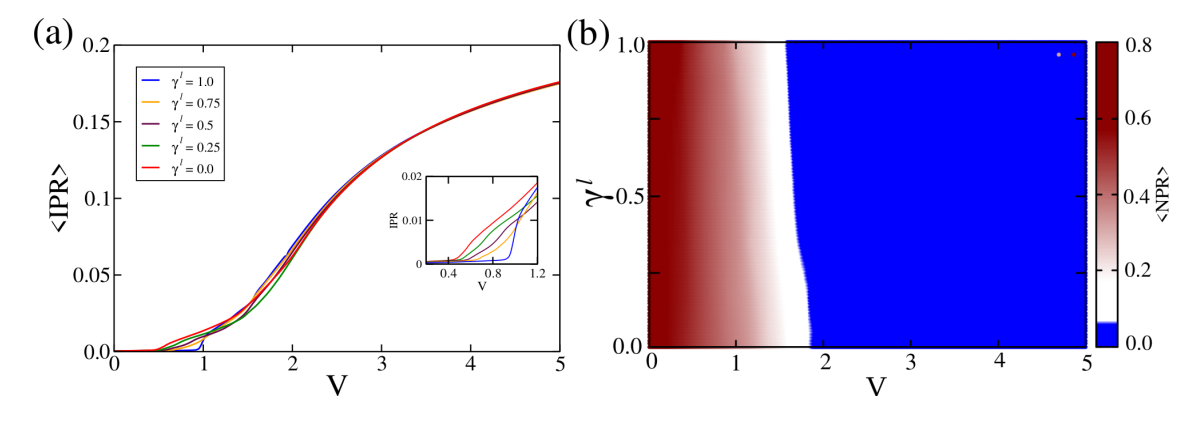


FIG. 5: (Color online). With dissipation applied at alternate site: (a) $\langle \text{IPR} \rangle$ as a function of the Aubry-André-Harper disorder strength V for $\gamma^l = 1, 0.75, 0.5, 0.25$, and 0, with fixed $\gamma^g = 1$ and system size 2N = 3000. (b) Phase diagram in the parameter space spanned by V and γ^l , where the color bar represents the $\langle \text{NPR} \rangle$. Here $\gamma^g = 1$ and the system size is 2N = 500.

When $\gamma^g = \gamma^l$, the system is in balanced gain-loss condition, while $\gamma^g \neq \gamma^l$ corresponds to an imbalanced regime. In Fig. 2, we plot average inverse participation ratio $(\langle IPR \rangle)$ and normalized participation ratio $(\langle NPR \rangle)$ as a function of disorder strength, V. Figure 2(a) represents the balanced gain-loss condition where $\gamma^g = \gamma^l = 1$. Here we can see that, a transition from a delocalized phase to a localized phase occurs at critical point V = 2. No mixed-phase region is observed, since there is no parameter range where both the $\langle IPR \rangle$ and $\langle NPR \rangle$ are simultaneously nonzero. This result is similar to a isolated AAH ladder where the transition occurs at $V/t = 2^{10}$. Now we introduce an imbalance in the system by taking the gain and loss dissipation strength as $\gamma^g = 1$ and $\gamma^l = 0.5$ which is shown in Fig. 2(b). This result indicate a delocalization to localization transition through a mixed-phase between V = 1.28 and V = 1.90 where both $\langle IPR \rangle$ and $\langle NPR \rangle$ are finite. In Fig. 2(c), we show the result for maximum imbalance condition where $\gamma^g = 1$ and $\gamma^l = 0$, i.e., only gain dissipation at alternate sites. Here mixed phase zone appears in between V = 0.98 and V = 1.87 which indicates that mixed-phase window increases with increasing the imbalanced dissipation in the system.

To obtain a complete picture of the delocalization to localization transition, In Fig. 3 we plot $\langle \text{IPR} \rangle$ and $\langle \text{NPR} \rangle$ by changing γ^l and keeping $\gamma^g = 1$. Figure 3(a) shows the variation of $\langle \text{IPR} \rangle$ with V for $\gamma^l = 1, 0.75, 0.5, 0.25, 0$

(blue, orrange, maroon, green, red). Here we can see that by decreasing γ^l and hence increasing imbalance between loss and gain, the critical value for phase transition from delocalized to mixed-phase zone gradually decreases, making the system easier to be localized. In Fig. 3(b), we display the $\langle \text{NPR} \rangle$ in the two-dimensional parameter space V versus γ^l , in which the color bar indicates the $\langle \text{NPR} \rangle$ values. Here we fix the system size 2N=500 and the red, white, and blue color zones represent delocalized, mixed and localized regime, respectively. When gradually increasing γ^l , mixed-phase zone decreases and the transition point from the mixed phase to the localized phase moves toward larger disorder strengths. At $\gamma^l=1$, the transition occurs at V/t=2.

B. Dissipation at alternate site

In this configuration, the Lindblad operators act only on every other site, arranged alternately as gain and loss described by

$$L_{p,j}^g = \sqrt{\gamma^g} c_{p,j}^{\dagger}; \quad \text{for } j = 1, 5, 9, \dots$$

$$L_{p,j}^l = \sqrt{\gamma^l} c_{p,j}; \quad \text{for } j = 3, 7, 11, \dots$$

In Fig. 4, we plot $\langle IPR \rangle$ and $\langle NPR \rangle$ as a function of V for three different values of γ^l keeping $\gamma^g = 1$. The balanced condition $(\gamma^g = \gamma^l = 1)$ is shown in Fig. 4(a). Unlike

previous case, this result shows that mixed-phase zone appear in between V=0.98 and V=1.78 even in balanced condition. With increasing the imbalance between gain and loss by decreasing γ^l to 0.5 which is shown in Fig. 4(b), the mixed phase zone increases and lying between V=0.75 and V=1.8. Figure 4(c) shows the result for maximum imbalance, with $\gamma^l=0$. In this case the transition from delocalization to localization phase occurs through mixed-phase window between V=0.56 and V=1.86. Here the width of the mixed-phase zone become maximum.

Now, like the previous case, to have a complete understanding of the role of dissipation, here we also plot $\langle IPR \rangle$ for five different values of γ^l and $\langle NPR \rangle$ for all possible values of γ^l as a function of V in Fig. 5(a) and Fig. 5(b) respectively. From the inset of Fig. 5(a) it is clear that, with decreasing γ^l i.e, increasing the imbalance the critical point for transition from delocalized to mixed-phase zone shifts gradually towards the lower disorder value. Figure 5(b) shows the dependence of $\langle NPR \rangle$ on V and γ^l , where the $\langle NPR \rangle$ values are indicated by the color bar. Here we keep system size 2N = 500. Red, white, and blue regions represent the delocalized, mixed, and localized regime respectively. This result indicates that the localization transition has a strong dependence on dissipation strength γ^l . With increasing γ^l the width of the mixed-phase zone decreases and the transition from the mixed phase to the localized phase occurs towards the lower disorder value. At balanced condition, i.e, for $\gamma^l = 1$ the critical point of transition occur at V/t = 1.57.

IV. CLOSING REMARKS

In this work, we have explored localization transition in a quasiperiodic ladder in presence of environmental dissipation. The quasiperiodicity is described by AAH model. Two different kinds of dissipation configurations have been taken into account. For one case, alternate gain and loss are applied to each site and for other case it has applied to every other site. The central focus of this work is to explore the interplay between dissipation and disorder on localization transition. A tight-binding model is employed to construct the Hamiltonian of the ladder, while the effect of dissipation is included using the Lindblad master equation formalism. The third quantization method within the Majorana fermionic representation has been used to calculate the damping matrix. The inverse and normalized participation ratios has been

- obtained from the damping matrix to analyze the localization phenomena. The key results of our work are as follows.
- (i) Dissipation induces a complex phase diagram comprising extended, mixed, and localized regimes without imposing any constraints on the hopping parameter or quasiperiodic potential. The critical points and mixed-phase zone can be tuned by varying the dissipation strength.
- (ii) For dissipation acting alternatively on all sites under balanced gain-loss conditions, the localization transition occurs at the same critical point as in the closed AAH ladder, and no mixed-phase region is observed. However, introducing gain-loss imbalance results in the appearance of a mixed-phase region, which progressively broadens with increasing imbalance.
- (iii) When alternating gain-loss dissipation is applied to every other sites, a mixed-phase region emerges even under perfectly balanced gain-loss conditions and the width of this mixed-phase zone increases with increasing imbalance.
- (iv) In both dissipation schemes, the critical disorder strength for the transition from the delocalized to the mixed phase shifts toward lower disorder values as the imbalance between gain and loss increases. In contrast, for the transition from the mixed to the localized phase, the critical disorder strength decreases with increasing imbalance in the case of dissipation at each site, whereas it increases for dissipation applied at every other site.

Our results reveal that dissipation can fundamentally reshape the localization properties of quasiperiodic AAH ladders, giving rise to tunable transitions between delocalized, mixed, and localized phases. Remarkably, such a mixed-phase regime can occur even without diagonal hopping or additional constraints on the quasiperiodic potential, highlighting dissipation as an effective control parameter for engineering phase transitions in non-Hermitian quasiperiodic systems.

ACKNOWLEDGMENTS

SS is thankful to ANRF, India (File number: PDF/2023/000319) for providing her research fellowship. SS acknowledges JNCASR, India for funding. SKP acknowledges the JC Bose fellowship and ANRF (File No. ANRF/JCB/SKP/4719), Govt. of India for the financial assistance. The authors thank Dr. Subhasis Sinha for useful discussions.

^{*} Electronic address: suparna@jncasr.ac.in; These authors contributed equally to this work.

[†] These authors contributed equally to this work.

[‡] Electronic address: pati@jncasr.ac.in

¹ P. W. Anderson, Absence of diffusion in certain random lattices. Phys. Rev. **109**, 1492 (1958).

² E. Abrahams, P. W. Anderson, D. C. Licciardello and T. V. Ramakrishnan, Scaling theory of localization: Absence

of quantum diffusion in two dimensions, Phys. Rev. Lett. 42, 673 (1979).

³ F. Evers and A. D. Mirlin, Anderson transitions, Rev. Mod. Phys. 80, 1355 (2008).

⁴ N. F. Mott, Electrons in disordered structures, Adv. Phys. 50, 865 (2001).

⁵ F. M. Izrailev, and A. A. Krokhin, Localization and the mobility edge in one-dimensional potentials with correlated

disorder, Phys. Rev. Lett. 82, 4062 (1999).

⁶ P. Carpena, P. Bernaola-Galván, P. C. Ivanov, and H. E. Stanley, Metal-insulator transition in chains with correlated disorder, Nature 418, 955 (2002).

- ⁷ P. G. Harper, The general motion of conduction electrons in a uniform magnetic field, with application to the diamagnetism of metals, Proc. R. Soc. Lond. Ser. A 68, 874 (1955).
- 8 S. Aubry and G. André, Analyticity breaking and Anderson localization in incommensurate lattices, Ann. Isr. Phys. Soc. 3, 133 (1980).
- ⁹ M. Rossignolo and L. Dell'Anna, Localization transitions and mobility edges in coupled Aubry-André chains, Phys.Rev.B 99, 054211 (2019).
- ¹⁰ S. Sil, S. K. Maiti, and A. Chakrabarti, Metal-Insulator Transition in an Aperiodic Ladder Network: An Exact Result, Phys. Rev. Lett. **101**, 076803 (2008).
- ¹¹ X. Deng, S. Ray, S. Sinha, G. V. Shlyapnikov, and L. Santos, One-dimensional quasicrystals with power-law hopping, Phys. Rev. Lett. **123**, 025301 (2019).
- ¹² N. Roy and A. Sharma, Fraction of delocalized eigenstates in the long-range Aubry-André-Harper model, Phys. Rev. B 103, 075124 (2021).
- ¹³ X.-C. Zhou, Y. Wang, T.-F. Poon, Q. Zhou, and X.-J. Liu, Exact new mobility edges between critical and localized states, Phys. Rev. Lett. 131, 176401 (2023).
- ¹⁴ S. Roy, T. Mishra, B. Tanatar, and S. Basu, Reentrant localization transition in a quasiperiodic chain, Phys. Rev. Lett. **126**, 106803 (2021).
- ¹⁵ S. Ganeshan, J. H. Pixley, and S. Das Sarma, Nearest neighbor tight binding models with an exact mobility edge in one dimension, Phys. Rev. Lett. 114, 146601 (2015).
- A. Padhan, M. Giri, S. Mondal, and T. Mishra, Emergence of multiple localization transitions in a one-dimensional quasiperiodic lattice, Phys. Rev. B 105, L220201 (2022).
- Y. Wang, X. Xia, L. Zhang, H. Yao, S. Chen, J. You, Q. Zhou, and X.-J. Liu, One-dimensional quasiperiodic mosaic lattice with exact mobility edges, Phys. Rev. Lett. 125, 196604 (2020).
- ¹⁸ N. G. V. Kampen, Stochastic Processes in Physics and Chemistry (North-Holland, Amsterdam, 1992).
- ¹⁹ M. Scully and M. S. Zubairy, *Quantum Optics* (Akademic, Berlin, 1996).
- ²⁰ P. Zanardi and M. Rasetti, Noiseless Quantum Codes, Phys. Rev. Lett. **79**, 3306 (1997).
- F. Verstraete, M. M. Wolf, and J. I. Cirac, Quantum computation and quantum-state engineering driven by dissipation, Nat. Phys. 5, 633 (2009).
- ²² S. Diehl, E. Rico, M. A. Baranov, and P. Zoller, Nat. Phys. **7**, 971 (2011).
- ²³ C. M. Bender, S. Boettcher, Real Spectra in Non-Hermitian Hamiltonians Having PT Symmetry, Phys. Rev. Lett. 80, 5243 (1998).
- ²⁴ T. Liu, S. Cheng, H. Guo, X. Gao, Fate of Majorana zero modes, exact location of critical states, and unconventional real-complex transition in non-Hermitian quasiperiodic lattices, Phys. Rev. B 103, 104203 (2021).
- ²⁵ H. Ramezani, T. Kottos, R. El-Ganainy, D. N. Christodoulides, Unidirectional nonlinear PT-symmetric optical structures. Phys. Rev. A 82, 043803 (2010).
- ²⁶ Q. -B. Zeng, S. Chen, and R. Lü, Anderson localization in the non-Hermitian Aubry-André-Harper model with physical gain and loss, Phys. Rev. A 95, 062118 (2017).
- ²⁷ T. E. Lee, Anomalous Edge State in a Non-Hermitian Lattice, Phys. Rev. Lett. **116**, 133903 (2016).
- ²⁸ S. Yao and Z. Wang, Edge States and Topological In-

- variants of Non-Hermitian Systems, Phys. Rev. Lett. 121, 086803 (2018).
- ²⁹ D. S. Borgnia, A. J. Kruchkov, R.-J. Slager, Non-Hermitian Boundary Modes, Phys. Rev. Lett. **124**, 056802 (2020).
- N. Okuma, K. Kawabata, K. Shiozaki, and M. Sato, Topological Origin of Non-Hermitian Skin Effects, Phys. Rev. Lett. 124, 086801 (2020).
- ³¹ C. M. Bender and S. Boettcher, Real Spectra in Non-Hermitian Hamiltonians Having PT Symmetry, Phys. Rev. Lett. 80, 5243 (1998).
- ³² K. Esaki, M. Sato, K. Hasebe, and M. Kohmoto, Edge states and topological phases in non-Hermitian systems, Phys. Rev. B 84, 205128 (2011).
- ³³ C. Yuce, Topological phase in a non-Hermitian PT symmetric system, Phys. Lett. A 379, 1213 (2015).
- ³⁴ S. Sarkar, S. Satpathi, and S. K. Pati, Enhancement of persistent current in a non-Hermitian disordered ring, Phys. Rev. B **112**, 035425 (2025).
- ³⁵ A. Mostafazadeh, Psedo-Hermitian representation of quantum mechanics, Int. J. Geom. Meth. Mod. Phys. 7, 1191 (2010).
- ³⁶ M. Znojil, Unitarity corridors to exceptional points, Phys. Rev. A **100**, 032124 (2019).
- ³⁷ A. Guo, G. J. Salamo, D. Duchesne, R. Morandotti, M. Volatier-Ravat, V. Aimez, G. A. Siviloglou, and D. N. Christodoulides, Observation of PT-Symmetry Breaking in Complex Optical Potentials, Phys. Rev. Lett. 103, 093902 (2009).
- A. Regensburger, C. Bersch, M.-A. Miri, G. Onishchukov, D. N. Christodoulides, and U. Peschel, Parity-time synthetic photonic lattices, Nature (London) 488, 167 (2012).
- ³⁹ L. Feng, M. Ayache, J. Huang, Y.-L. Xu, M.-H. Lu, Y.-F. Chen, Y. Fainman, and A. Scherer, Nonreciprocal Light Propagation in a Silicon Photonic Circuit, Science 333, 729 (2011).
- ⁴⁰ C. M. Bender, B. K. Berntson, D. Parker, and E. Samuel, Observation of *PT* phase transition in a simple mechanical system Am. J. Phys. 81, 173 (2013).
- ⁴¹ J. Schindler, A. Li, M. C. Zheng, F. M. Ellis, and T. Kottos, Experimental study of active LRC circuits with PT symmetries Phys. Rev. A 84, 040101(R) (2011).
- ⁴² C. Mejía-Cortés and M. I. Molina, Interplay of disorder and PT symmetry in one-dimensional optical lattices, Phys. Rev. A 91, 033815 (2015).
- ⁴³ D. M. Jović, C. Denz, and M. R. Belić, Anderson localization of light in *PT*-symmetric optical lattices, Opt. Lett. 37, 4455 (2012).
- ⁴⁴ C. Yuce, PT symmetric Aubry–Andre modelPhys. Lett. A 378, 2024 (2014).
- ⁴⁵ C. H. Liang, D. D. Scott, and Y. N. Joglekar, PT restoration via increased loss and gain in the PT-symmetric Aubry-André model Phys. Rev. A 89, 030102(R) (2014).
- ⁴⁶ H. J. Carmichael, Quantum Trajectory Theory for Cascaded Open Systems, Phys. Rev. Lett. **70**, 2273 (1993).
- ⁴⁷ Y. Ashida, Z. Gong, and M. Ueda, Non-Hermitian physics, Adv. Phys. **69**, 3 (2020).
- ⁴⁸ H. Weimer, A. Kshetrimayum, and R. Orús, Simulation methods for open quantum many-body systems, Rev. Mod. Phys. 93, 015008 (2021).
- ⁴⁹ G. Lindblad, On the generators of quantum dynamical semigroups, Commun. Math. Phys. **48**, 119 (1976).
- ⁵⁰ H.-P. Breuer and F. Petruccione, The Theory of Open Quantum Systems, Oxford University Press (2007).
- ⁵¹ H. J. Carmichael, Quantum Trajectory Theory for Cascaded Open Systems, Phys. Rev. Lett. **70**, 2273 (1993).

- J. Dalibard, Y. Castin, and K. Mølmer, Wave-Function Approach to Dissipative Processes in Quantum Optics, Phys. Rev. Lett. 68, 580 (1992).
- T. Prosen, Third quantization: A general method to solve master equations for quadratic open Fermi systems, New J. Phys. 10, 043026 (2008).
- ⁵⁴ T. Prosen and B. Žunkovič, Exact solution of Markovian master equations for quadratic Fermi systems: Thermal
- baths, open XY spin chains and non-equilibrium phase transition, New J. Phys. **12**, 025016 (2010).
- T. Prosen, Spectral theorem for the Lindblad equation for quadratic open fermionic systems, J. Stat. Mech. (2010) P07020.
- ⁵⁶ T. Li , Y. -S. Zhang, and W. Yi, Engineering dissipative quasicrystals, Phys. Rev. B 105, 125111 (2022).